

Process Oriented Diagnostics of Tropical Cyclones in Climate Models

1. General Information

1.1 Award details

- Award Number: NA15OAR4310087
- Program Officer: Daniel Barrie ,301-734-1256, Daniel.Barrie@noaa.gov
- Program Office: OAR Climate Program Office (CPO)
- Award Period: 08/01/2015 - 07/31/2018
- Project Title: Process Oriented Diagnostics of Tropical Cyclones in Climate Models
- Recipient Name: University of Washington
- PIs/PDs: Daehyun Kim

1.2 Report details

- Report Type: Project Progress Report
- Reporting Period: 08/01/2015 - 07/31/2018
- Final Report: Yes

2. Main Goals of the project

- 1) Analyze the relationship of the large-scale environment to tropical cyclone (TC) activity in a suite of global models, including both high-resolution global atmospheric models and CMIP5 coupled climate models.
- 2) Develop and apply process-based diagnostics to analyze the differences in model characteristics that are relevant to the model performance in simulating TCs.
- 3) Analyze the relationship of wave disturbances to TCs in climate models.
- 4) Make modifications to the physics of the GISS model based on the results of item #2 and determine the sensitivity of the model TC characteristics to those changes.

3. Results and accomplishments

The current report summarizes the results and accomplishments from the research activity of the University of Washington researchers.

3.1 Development of process-oriented TC diagnostics

Our project started from the knowledge that there are some similarities between the processes involved in tropical cyclogenesis and those in the Madden-Julian Oscillation (MJO). We made necessary and major modifications to diagnostics which were originally developed for the MJO to yield a set of process-oriented diagnostics for TCs (Kim et al. 2018). No widely-accepted such process-based diagnostics for global TC modeling existed before our project.

The developed process-oriented TC diagnostics aim to characterize the moist thermodynamics of TCs. The diagnostics described in Kim et al. (2018) focuses on how convection, moisture, clouds and related processes are coupled at individual grid points, and

yields information about how the convective parameterizations interact with resolved model dynamics around simulated TC centers.

Our diagnostics was inspired by the diagnostics that have been used in the MJO community and aim to examine the couplings between physical processes at the GCM grid scale. Diagnostics such as those relating free-tropospheric humidity to precipitation at daily time scales and individual grid points, for example, show great diversity across multi-model ensembles, and have shown power in explaining MJO simulation quality across those ensembles (e.g., Kim et al. 2011, 2014). Our project applied similar diagnostics to the problem of TC simulation in global models.

We targeted azimuthally averaged TC structure, which is well-documented and well-understood. The diagnostics produce a series of composite diagrams of azimuthally-averaged variables around TC centers as a function of TC intensity. Unlike in the MJO diagnostics, in which daily-averaged values are used, our TC diagnostics use 6- or 3-hourly datasets. It is important that the model-to-model or model-to-observation comparison be made using TCs at a similar intensity because the TC structures show dependency on TC intensity. We determined the intensity values at which the model-to-model comparison was made using the azimuthally-averaged maximum near-surface wind speed (WS_{max}) and used the term 'stage' to indicate a given intensity range (e.g., Figure 1).

Tangential, radial and pressure velocity, warm-core temperature, and relative humidity were used to examine wind and thermodynamic TC structures (e.g., Figures 2-4). The co-variability between precipitation and precipitable water/column relative humidity was analyzed to assess the moisture-convection coupling within the TCs (e.g., Figures 5-7). The surface turbulent fluxes and surface and top-of-atmosphere (TOA) radiative fluxes were examined to evaluate the surface enthalpy flux feedback and the cloud-radiation feedback (e.g., Figures 8-9).

3.2 Application of the process-oriented TC diagnostics to a suite of climate model simulations

a) List of model simulations

Our process-oriented TC diagnostics have been used to evaluate the target processes in eight GCM simulations (Table 1). They can be grouped into three subsets, based on the horizontal grid spacing used in the simulations – 0.25° , 0.5° , and 1.0° resolution.

- 0.25° simulations

Two of the three GCM simulations at 0.25° resolution are from the atmosphere-only NCAR/DOE Community Atmospheric Model (CAM) version 5 using two different dynamical cores – finite volume (FV: Lin 2004; Neale et al. 2012) and spectral element (SE: Dennis et al. 2012). Hereafter, they will be referred to as the CAM5fv and CAM5se simulations, respectively. The CAM5fv simulation uses a globally uniform 0.25° horizontal grid spacing (e.g., Wehner et al. 2014), but the CAM5se simulation uses a variable-resolution horizontal grid, with 0.25° grid only over the North Atlantic region and 1° resolution elsewhere (e.g., Zarzycki and Jablonowski 2014; Zarzycki et al. 2017). The main difference between the CAM5se and CAM5fv simulations lies in the dynamical core, which has been shown to influence the simulation of TC activity (Reed et al. 2015). The CAM5se and CAM5fv simulations are performed for 1992-1999 and 1996-1997, respectively.

The other 0.25° simulation is performed with the Centro Euro-Mediterraneo sui Cambiamenti Climatici (CMCC) Climate Model version 2 (e.g., Fogli and Iovino 2014; Scoccimarro et al. 2017). Its atmospheric component is the NCAR/DOE CAM version 5 (Hurrell et al. 2013) that uses a globally uniform 0.25° horizontal grid spacing and 30 vertical levels. Its ocean component is the NEMO ocean general circulation model version 3.4 (Madec et al. 2008) that has the 0.25° horizontal resolution and 50 levels in the vertical, with 22 levels representing the upper 100 meters of the ocean. Hereafter, this will be referred to as the CMCC simulation. The CMCC simulation covers 1958-1959.

- 0.5° simulations

Two of the three 0.5° simulations are from atmosphere-only GCMs: The Geophysical Fluid Dynamics Laboratory Atmospheric Model version 2.5 (AM2.5; Delworth et al. 2012) and High Resolution Atmospheric Model (HiRAM; Zhao et al. 2009). The other simulation is from a coupled atmosphere-ocean GCM: the Forecast-oriented Low Ocean Resolution (FLOR; Vecchi et al. 2014) version of Coupled Model 2.5 (CM2.5; Delworth et al. 2012). The atmospheric components of the AM2.5 and FLOR models are identical. All three models use the same NOAA Geophysical Fluid Dynamics (GFDL) finite volume dynamical core on a cubed sphere horizontal grid (Putman and Lin 2007) but have different physics parameterizations and ocean models. The AM2.5 and FLOR models use a relaxed Arakawa-Schubert deep convection scheme (Moorthi and Suarez 1992), while the HIRAM model uses a shallow convection scheme of Bretherton et al. (2004) that has been modified to simulate both deep and shallow clouds (Zhao et al. 2012). All three models have the identical 32 vertical levels, and simulations are performed for two years between 1984-1985.

- 1.0° simulations

There are two 1° resolution time-slice simulations whose output are made available for the NOAA Model Diagnostics Task Force (MDTF) project – the NCAR CAM 5.3 and GFDL AM4 models. Both models are atmosphere-only GCMs, so the simulations are AMIP type, with prescribed sea surface temperature and sea ice as lower boundary conditions. The NCAR CAM5 model has 30 vertical levels, and the GFDL AM4 model has 32 vertical levels. The NCAR CAM5 and GFDL AM4 simulations are performed for 1990-1994 and 2008-2012, respectively. Hereafter, the MDTF NCAR CAM version 5.3 (Neale et al. 2012) and GFDL AM4 model (Zhao et al. 2018a,b) simulations will be referred to as the NCARts and GFDLts.

b) Results of the multi-model analysis

Figure 1 shows intensity distributions of all TCs detected in the GCM simulations. Our results showed that, although stronger TCs are more frequent in higher-resolution GCM simulations, as has been noted in many previous, there are considerable variations in intensity distributions even at similar horizontal resolutions (e.g., HIRAM vs. AM2.5 and CMCC vs. CAM5fv).

The TC wind fields in the models share many similarities with observed TCs (Figures 2 and 3) and using smaller horizontal grid spacing leads to better representation of vertical velocity near the TC center. The location of peak upward motion (i.e., the most negative omega values) appears to move away from the storm center as horizontal resolution increases (i.e., going from the bottom to top panels in Figure 3). Overall, we found that the three-dimensional wind and warm-core structures of simulated TCs with horizontal resolution show a systematic resolution dependence.

One of the main findings of our study is that while the wind structures of in the inner-core regions of TCs seem to be strongly constrained by horizontal resolution of the models (Figures 2-3), their thermodynamics structures appears to be less affected by horizontal resolution (Figures 4-9), suggesting that model parameterizations are what determines the themodynamic structures of TCs. The distributions of relative humidity (Figure 4), precipitation (Figure 5), column moisture and column relative humidity (Figures 6-7), surface and radiative fluxes (Figure 8-9) around TCs do not exhibit any significant systematic variations with horizontal resolution, except in those that are strongly controlled by the locations of the Radius of Maximum Winds and peak rising motions near the TC center. They remained diverse across the models with similar horizontal resolutions. This suggests that thermodynamic structures of TCs could be partly responsible for the inter-model diversity of TC intensity in GCM simulations.

Another main finding of our study is that models that produce a greater amount of rainfall in the inner-core regions tended to simulate stronger TCs more frequently (Figure 10, also in Kim et al. 2018). This relationship was noted among the simulations with comparable horizontal resolution (Kim et al. 2018), as well as across all of the simulations examined (Moon et al. in preparation). Figure 10 shows a scatterplot of the area-averaged inner-core rainfall rates at 12-15 ms^{-1} vs. the fraction of TCs intensifying from 12 ms^{-1} to 18 ms^{-1} for all TCs simulated in the GCM simulations. The scatterplot shows a clear positive correlation between the inner-core rainfall rates and intensification probability at comparable horizontal resolutions (diamonds, squares, and circles for the 0.25°, 0.5°, and 1.0° simulations), and there appears to be a good positive correlation between them across all of the simulations. These high positive correlations are consistent with previous theoretical studies that found greater diabatic heating near the TC center to be favorable for TC intensification.

We also found that the magnitude of the surface heat flux was greater than the column radiative flux convergence, but the radial gradient of the net column radiative flux convergence was comparable to that of surface turbulent heat flux for weak TCs (Figures 8 and 9), which highlighted the importance of cloud-radiative feedbacks during the early developmental phases of TCs. This is consistent with Wing et al. (2016; 2018), who performed an MSE variance budget analysis of TC formation and intensification, in which the surface heat flux and radiative flux convergence are two of the budget terms. Models that produce a greater amount of rainfall in the inner-core regions tended to simulate stronger TCs more frequently, as in Kim et al. (2018), which are consistent with previous theoretical studies.

We plan to submit a manuscript containing the results summarized above in the Fall of 2018 to Journal of Climate (Moon et al., in preparation).

The UW team has also been actively engaged in the development of TC genesis diagnostics (Wing et al. 2018) that are based on moist static energy variance budget (Wing and Emanuel 2014).

3.3. Contribution to the NOAA MAPP MDTF activity

We have started converting our codes that produce the process-oriented TC diagnostics into an open-source language (Python/NCL). Parts of the scripts used for these diagnostics (e.g., Figure 5) have been included in the NOAA MAPP MDTF diagnostics suite.

We have also contributed with a summary of these results to the NOAA MAPP MDTF BAMS manuscript (Maloney et al. 2018).

4. Highlights of Accomplishments

- We have developed process-oriented diagnostics for TCs by adapting diagnostics that were originally developed for the Madden-Julian Oscillation (Kim et al. 2018). No widely-accepted such process-based diagnostics for global TC modeling existed before our project.
- The diagnostics we developed have been applied to eight climate model simulations, including those of six high-resolution models and two NOAA MAPP MDTF simulations, which has allowed us to identify processes that are key to TC intensification (Kim et al. 2018; Moon et al. in preparation).
- Key results from our model diagnosis includes:
 - models with higher TC inner-core rainfall rates tend to produce stronger TCs at various resolutions.
 - thermodynamic structures of TCs are more loosely constrained by horizontal resolution than wind structures are
- We have contributed to the NOAA MAPP MDTF activity by having developed TC diagnostics scripts for MDTF diagnostics package and by having provided a figure and a paragraph to the BAMS article (Maloney et al., submitted).

5. Publications from the project

5.1 Manuscripts

- Kim, D., Y. Moon, S.J. Camargo, A.A. Wing, A.H. Sobel, H. Murakami, G.A. Vecchi, M. Zhao and E. Page, 2018. Process-oriented diagnosis of tropical cyclones in high-resolution GCMs. *J. Climate*, **31**, 1685-1702, doi: 10.1175/JCLI-D-17-0269.1.
- Wing, A.A., S.J. Camargo, A.H. Sobel, D. Kim, H. Murakami, K.A. Reed, G. A. Vecchi, M.F. Wehner, C. Zarzycki, and M. Zhao, 2018: Moist static energy budget analysis of tropical cyclones in climate models, submitted to *Journal of Climate*.
- Moon, Y., D. Kim, S. Camargo, A. Wing, A. Sobel, H. Murakami, K. Reed, G. Vecchi, M. Wehner, C. Zarzycki, and M. Zhao: Wind and thermodynamic structures of tropical cyclones and their sensitivity to horizontal resolution in global climate models. *J. Climate*, In preparation.

5.2 Conferences and workshop contributions

- S.J. Camargo, D. Kim, A.A. Wing, A.H. Sobel, H. Murakami, E. Scoccimarro, M. Zhao and G.A. Vecchi, 2016. Process oriented diagnostics of tropical cyclones in climate models. 32nd American Meteorological Society Conference on Hurricanes and Tropical Meteorology. 17-22 April 2016, San Juan, Puerto Rico, oral presentation by S. Camargo.
- S.J. Camargo, D. Kim, Y. Moon, A.H. Sobel, A.A. Wing, H. Murakami, K.A. Reed, E. Scoccimarro, G.A. Vecchi, M.F. Wehner, C.M. Zarzycki, and M. Zhao, 2016. Process oriented diagnostics of tropical cyclones in climate models. Fall Meeting AGU, Abstract A13L-04, San Francisco, CA, 12-16 December 2016, oral presentation by S. Camargo.

- D. Kim, S. J. Camargo, Y. Moon, A. H. Sobel, A. A. Wing, H. Murakami, E. Scoccimarro, G. A. Vecchi, C. M. Zarzycki, and M. Zhao, 2017. Process oriented diagnostics of tropical cyclones in climate models. Abstract 10.3. 29th Conference on Climate Variability and Change, 97th American Meteorological Society Annual Meeting, January 22-26, 2017, Seattle, WA, oral presentation by D. Kim.
- Wing, A.A., S.J. Camargo, A. Sobel, D. Kim, H. Murakami, K. Reed, G. Vecchi, M. Wehner, C. Zarzycki, and M. Zhao, 2017. Comparison of tropical cyclogenesis processes in climate model and cloud-resolving model simulations using moist static energy budget analysis. Geophys. Res. Abstracts, 19, EGU2017-11207, EGU General Assembly 2017, 23-28 April 2017, Vienna, Austria, oral presentation by A. Wing.
- Moon, Y., D. Kim, S.J. Camargo, A.A. Wing, A.H. Sobel, H. Murakami, K.A. Reed, G.A. Vecchi, C.M. Zarzycki, and M. Zhao, 2017: Process-Oriented Diagnostics of Tropical Cyclones in Global Climate Models. 5th WGNE workshop on systematic errors in weather and climate models, Montreal, Quebec, Canada, June 19-23, 2017, poster presentation by Y. Moon.
- Moon, Y., D. Kim, S.J. Camargo, A.A. Wing, A.H. Sobel, M.G. Bosilovich, H. Murakami, K.A. Reed, G.A. Vecchi, M.F. Wehner, C.M. Zarzycki, and M. Zhao, 2017. Process-Oriented Diagnostics of Tropical Cyclones in Global Climate Models. Fall Meeting AGU, Abstract A13H-2212, New Orleans, LA, 11-15 December 2017, poster presentation by Y. Moon.
- Wing, A.A., S.J. Camargo, A.H. Sobel, D. Kim, Y. Moon, M.G. Bosilovich, H. Murakami, K.A. Reed, G.A. Vecchi, M.F. Wehner, C.M. Zarzycki, and M. Zhao, 2017. Moist Thermodynamics of Tropical Cyclone Formation and Intensification in High-Resolution Climate Model. Fall Meeting AGU, Abstract A11S-04, New Orleans, LA, 11-15 December 2017, oral presentation by A. Wing.
- Moon, Y., D. Kim, S.J. Camargo, A.A. Wing, A.H. Sobel, M.G. Bosilovich, H. Murakami, K.A. Reed, E. Scoccimarro, G.A. Vecchi, M.F. Wehner, C.M. Zarzycki, and M. Zhao, 2018: Process-oriented diagnostics of tropical cyclones in global climate models. 33rd Conference on Hurricanes and Tropical Meteorology, American Meteorological Society, April 16-20, 2018, Ponte Vedra, FL, poster presentation by D. Kim.
- Wing, A.A., S.J. Camargo, A.H. Sobel, D. Kim, Y. Moon, M. Bosilovich, H. Murakami, K.A. Reed, E. Scocci-marro, G.A. Vecchi, M.F. Wehner, C.M. Zarzycki, and M. Zhao, 2018. Abstract 9C.5. Moist Thermodynamics of Tropical Cyclone Formation and Intensification in High-Resolution Climate Models. 33rd Conference on Hurricanes and Tropical Meteorology, American Meteorological Society, April 16-20, 2018, Ponte Vedra, FL, oral presentation by A. Wing.
- Moon, Y., D. Kim, S.J. Camargo, A.A. Wing, A.H. Sobel, M.G. Bosilovich, H. Murakami, K.A. Reed, E. Scoccimarro, G.A. Vecchi, M.F. Wehner, C.M. Zarzycki, and M. Zhao, 2018: Process-oriented diagnostics of tropical cyclones in global climate models. 8th GEWEX Open Science Conference: Extremes and Water on the edge, May 6-11, 2018, Canmore, Alberta, Canada, oral presentation by Y. Moon.

6. PI Contact Information

Daehyun Kim
University of Washington
Department of Atmospheric Sciences, Box 351640
University of Washington, Seattle, WA 98195-1640
Tel: 206-221-8935
Email: daehyun@uw.edu

References

- Bretherton, C.S., J.R. McCaa, and H. Grenier, 2004: A New Parameterization for Shallow Cumulus Convection and Its Application to Marine Subtropical Cloud-Topped Boundary Layers. Part I: Description and 1D Results. *Mon. Wea. Rev.*, **132**, 864–882.
- Delworth, T.L., and Coauthors: 2012: Simulated Climate and Climate Change in the GFDL CM2.5 High-Resolution Coupled Climate Model. *J. Climate*, **25**, 2755–2781.
- Dennis, J. M., and Coauthors, 2012: CAM-SE: A scalable spectral element dynamical core for the Community Atmosphere Model. *International Journal of High Performance Computing Applications*, **26**, 74-89.
- Fogli, P. G. and D. Iovino, 2014: CMCC–CESM–NEMO: Toward the New CMCC Earth System Model. CMCC Research Paper No. 248.
- Hurrell, J.W., and Coauthors, 2013: The Community Earth System Model: A Framework for Collaborative Research. *Bull. Amer. Meteor. Soc.*, **94**, 1339–1360.
- Kim, D., A. H. Sobel, E. D. Maloney, D. M. W. Frierson, and I.-S. Kang, 2011: A Systematic Relationship between Intraseasonal Variability and Mean State Bias in AGCM Simulations. *J. Clim.*, **24**, 5506–5520.
- Kim, D., and Coauthors, 2014: Process-Oriented MJO Simulation Diagnostic: Moisture Sensitivity of Simulated Convection. *J. Clim.*, **27**, 5379–5395.
- Kim, D., Y. Moon, S.J. Camargo, A.A. Wing, A.H. Sobel, H. Murakami, G.A. Vecchi, M. Zhao and E. Page, 2018. Process-oriented diagnosis of tropical cyclones in high-resolution GCMs. *J. Climate*, **31**, 1685-1702.
- Lin, S., 2004: A “Vertically Lagrangian” Finite-Volume Dynamical Core for Global Models. *Mon. Wea. Rev.*, **132**, 2293–2307.
- Madec, G., and Coauthors, 2008: NEMO ocean engine version 3.0. Institut Pierre-Simon Laplace Rep. 27, 209 pp.
- Moon, Y., D. Kim, S. Camargo, A. Wing, A. Sobel, H. Murakami, K. Reed, G. Vecchi, M. Wehner, C. Zarzycki, and M. Zhao: Wind and thermodynamic structures of tropical cyclones and their sensitivity to horizontal resolution in global climate models. *J. Climate*, In preparation.
- Moorthi, S. and M.J. Suarez, 1992: Relaxed Arakawa-Schubert. A Parameterization of Moist Convection for General Circulation Models. *Mon. Wea. Rev.*, **120**, 978–1002.
- Putman, W. M., S.-J. Lin, 2007: Finite-volume transport on various cubed-sphere grids. *Journal of Computational Physics*, **227**, 55-78.
- Reed, K. A., J. T. Bacmeister, N. A. Rosenbloom, M. F. Wehner, S. C. Bates, P. H. Lauritzen, J. E. Truesdale, and C. Hannay, 2015: Impact of the dynamical core on the direct simulation of

- tropical cyclones in a high-resolution global model. *Geophys. Res. Lett.*, **42**, 3603–3608. doi:10.1002/2015GL063974.
- Scoccimarro, E., P.G. Fogli, K.A. Reed, S. Gualdi, S. Masina, and A. Navarra, 2017: Tropical Cyclone Interaction with the Ocean: The Role of High-Frequency (Subdaily) Coupled Processes. *J. Climate*, **30**, 145–162.
- Vecchi, G.A., and Coauthors: 2014: On the Seasonal Forecasting of Regional Tropical Cyclone Activity. *J. Climate*, **27**, 7994–8016.
- Wehner, M. F., and Coauthors, 2014: The effect of horizontal resolution on simulation quality in the Community Atmospheric Model, CAM5.1, *J. Adv. Model. Earth Syst.*, **6**, 980–997.
- Wing, A. A., and K. A. Emanuel, 2014: Physical mechanisms controlling self-aggregation of convection in idealized numerical modeling simulations. *J. Adv. Model. Earth Syst.*, **6**, 59–74.
- Wing, A.A., S.J. Camargo, and A.H. Sobel, 2016: Role of Radiative–Convective Feedbacks in Spontaneous Tropical Cyclogenesis in Idealized Numerical Simulations. *J. Atmos. Sci.*, **73**, 2633–2642.
- Wing, A. A., and Coauthors: 2018: Moist static energy budget analysis of tropical cyclone formation and intensification in high-resolution climate models. *J. Climate*, submitted.
- Zarzycki, C. M., and C. Jablonowski, 2014: A multidecadal simulation of Atlantic tropical cyclones using a variable-resolution global atmospheric general circulation model, *J. Adv. Model. Earth Syst.*, **6**, 805–828.
- Zarzycki, C. M., Reed, K. A., Bacmeister, J. T., Craig, A. P., Bates, S. C., and Rosenbloom, N. A., 2016: Impact of surface coupling grids on tropical cyclone extremes in high-resolution atmospheric simulations, *Geosci. Model Dev.*, **9**, 779–788.
- Zarzycki, C. M., D. R. Thatcher, and C. Jablonowski, 2017: Objective tropical cyclone extratropical transition detection in high-resolution reanalysis and climate model data, *J. Adv. Model. Earth Syst.*, **9**, 130–148.
- Zhao, M., I.M. Held, S. Lin, and G.A. Vecchi, 2009: Simulations of Global Hurricane Climatology, Interannual Variability, and Response to Global Warming Using a 50-km Resolution GCM. *J. Climate*, **22**, 6653–6678.
- Zhao, M., and Coauthors, 2018a: The GFDL global atmosphere and land model AM4.0/LM4.0: 1. Simulation characteristics with prescribed SSTs. *Journal of Advances in Modeling Earth Systems*, **10**, 691–734.
- Zhao, M., and Coauthors, 2018b: The GFDL global atmosphere and land model AM4.0/LM4.0: 2. Model description, sensitivity studies, and tuning strategies. *Journal of Advances in Modeling Earth Systems*, **10**, 735–769.

Simulation Name (Short Name)	Horizontal Resolution	Vertical Levels	Simulation Years	Ocean Coupling
NCAR CAM5 SE (CAM5se)	0.25° N. Atlantic only	30	1996-1997	No
NCAR CAM5 FV (CAM5fv)	0.25°	30	1992-1999	No
CMCC CM2 (CMCC)	0.25°	30	1958-1959	Yes
GFDL AM2.5 (AM2.5)	0.5°	32	1984-1985	No
GFDL FLOR (FLOR)	0.5°	32	1984-1985	Yes
GFDL HiRAM (HiRAM)	0.5°	32	1984-1985	No
MDTF NCAR CAM5 (NCARts)	1°	30	1990-1994	No
MDTF GFDL AM4 (GFDLts)	1°	32	2008-2012	No

Table 1: A summary of the eight GCM simulations analyzed during our project.

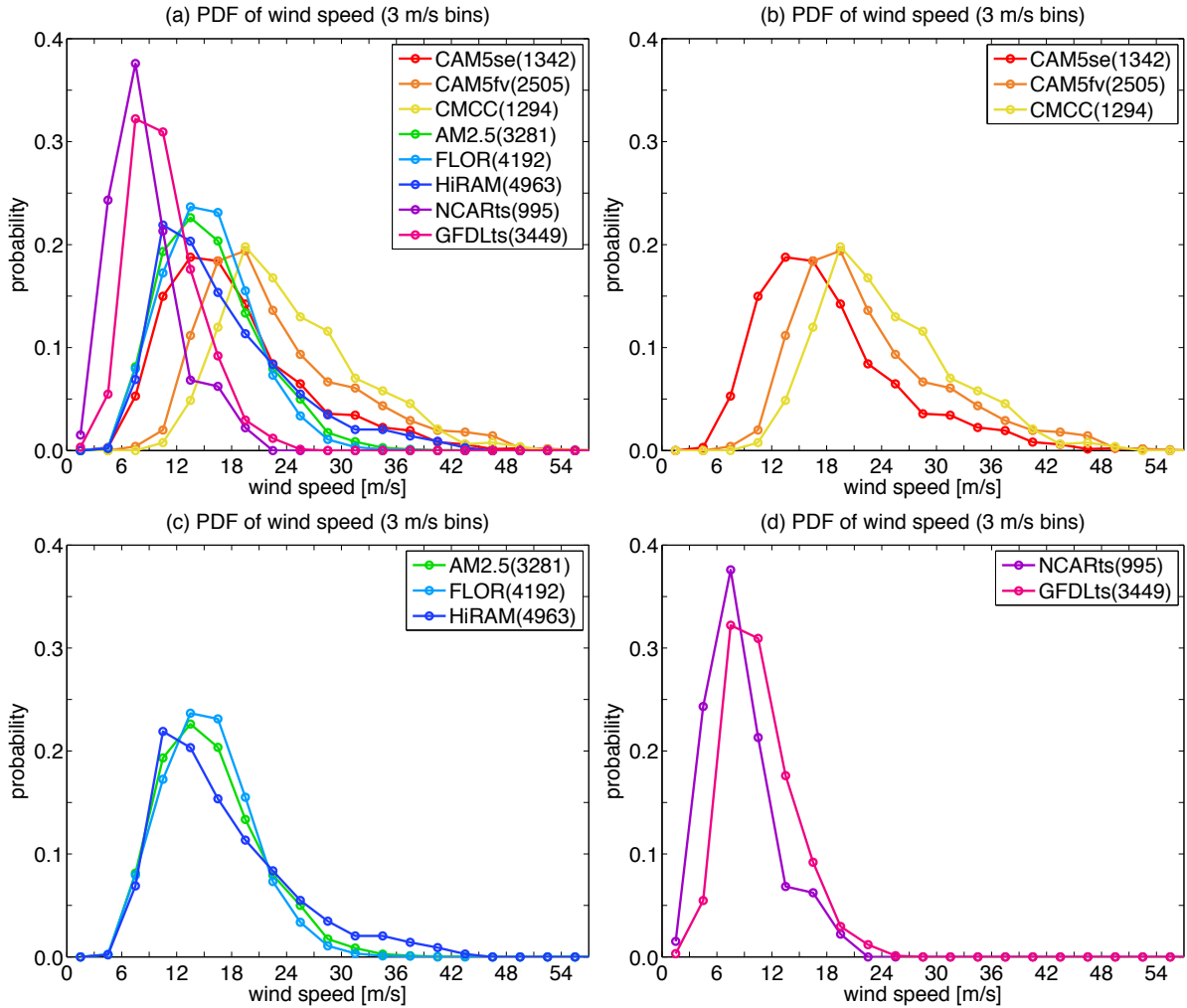


Figure 1: (a) Probability distribution curves of intensity of all tropical cyclones detected in the simulations. (b)-(d) are the same as in (a), but only showing 0.25°, 0.5°, and 1° degree resolution simulations only.

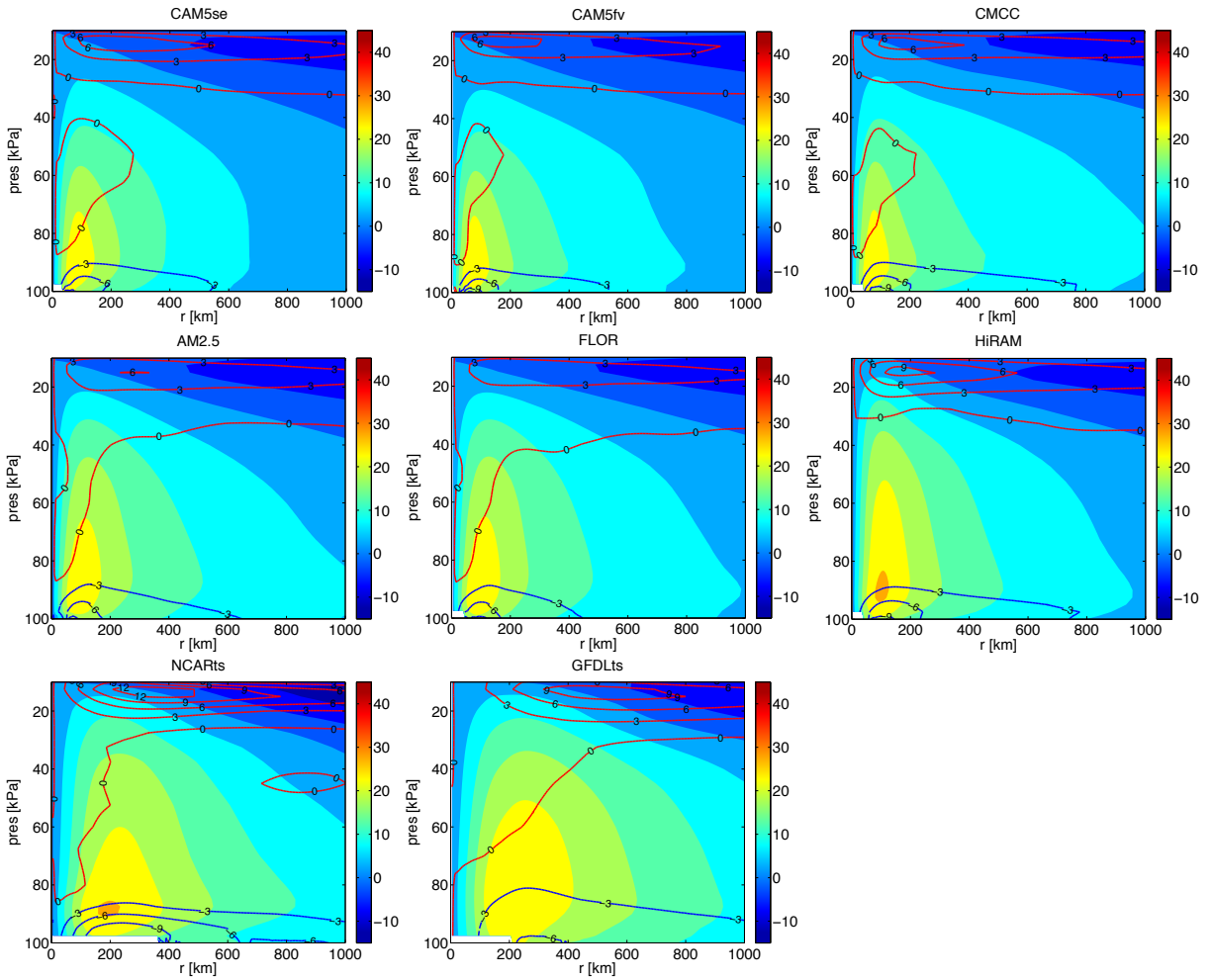


Figure 2: Radius-pressure plots of azimuthally averaged tangential velocity (shading) and radial velocity (lines), for all TC snapshots that have the intensity of $18\text{-}21\text{ m s}^{-1}$. The top, middle, and bottom rows are the 0.25° , 0.5° , and 1° simulations, respectively. Positive and negative lines are plotted in red and blue at 3 m s^{-1} intervals. Units are m s^{-1} .

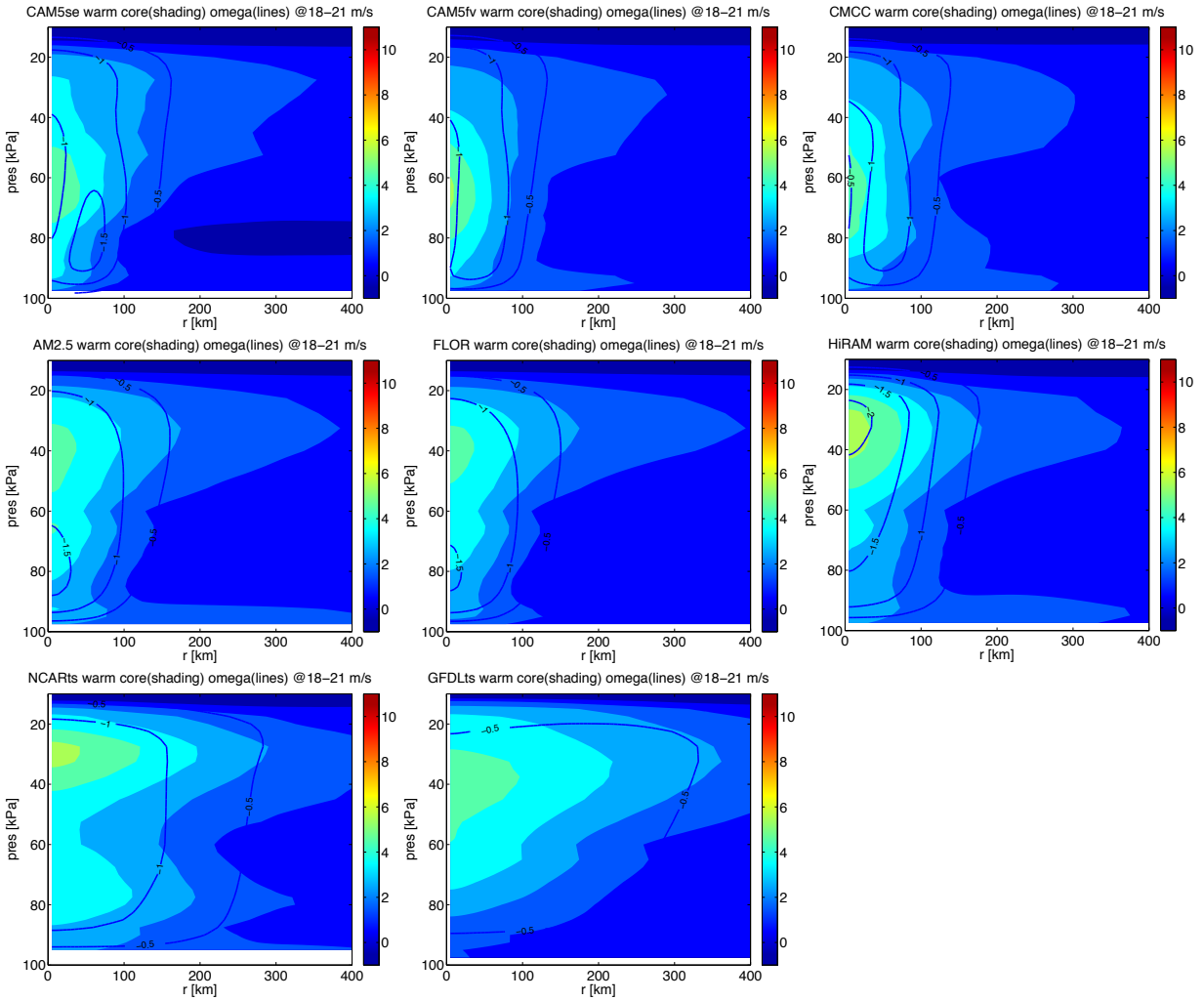


Figure 3: Same as in Figure 2, but for warm-core temperature anomalies (shading) and pressure velocity (lines). Negative lines are plotted in blue at 0.5 Pa s^{-1} intervals. Units are K for warm-core temperature anomalies and for Pa s^{-1} pressure velocity. Warm-core temperature anomalies are departures from the environment, which is the average of a TC-centered 2000-km square but excluding its inner 1000-km square area.

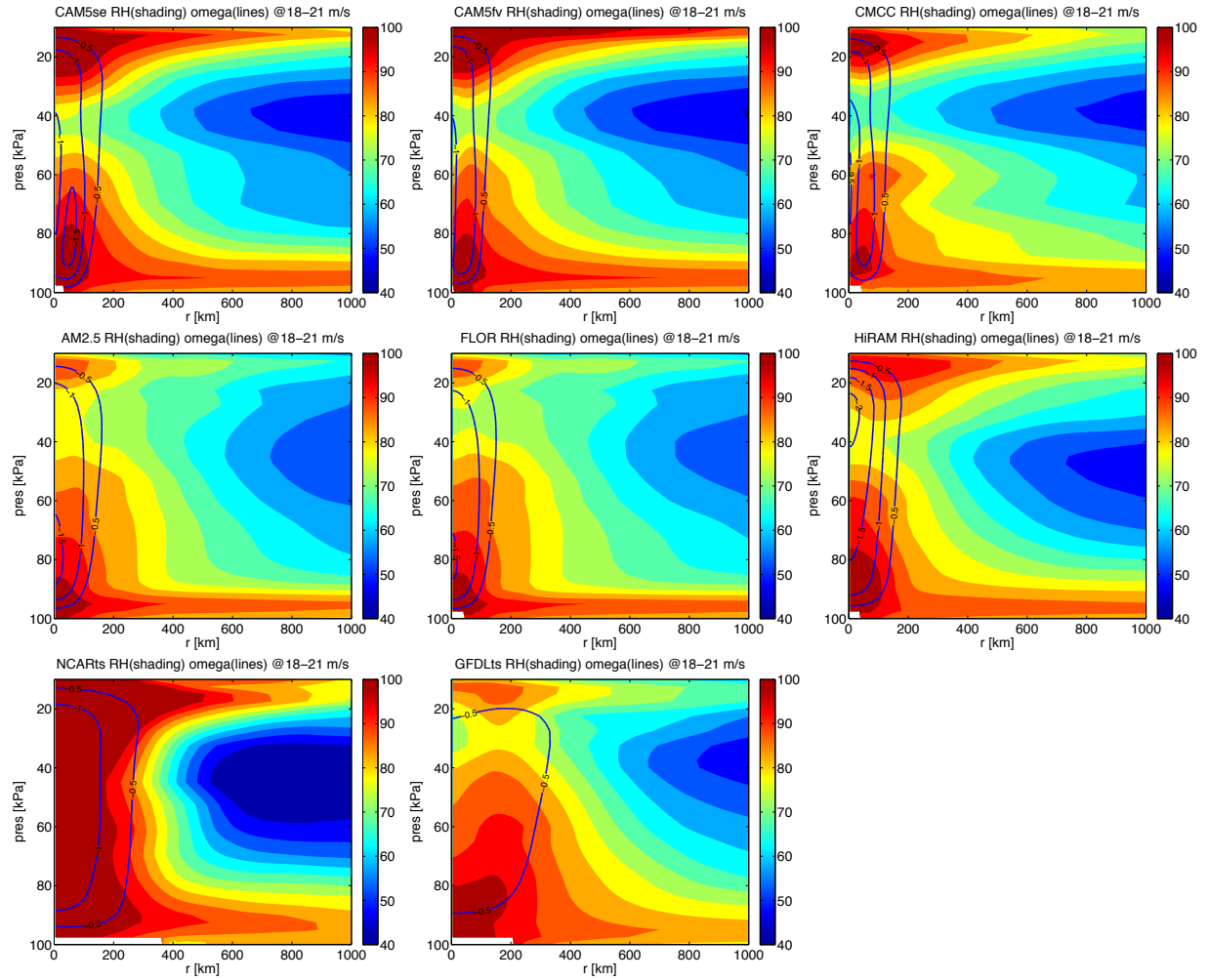


Figure 4: Same as in Figure 2, but for relative humidity (shading) and pressure velocity (lines). Negative lines are plotted in blue at 0.5 Pa s^{-1} intervals. Units are % for relative humidity and Pa s^{-1} for pressure velocity.

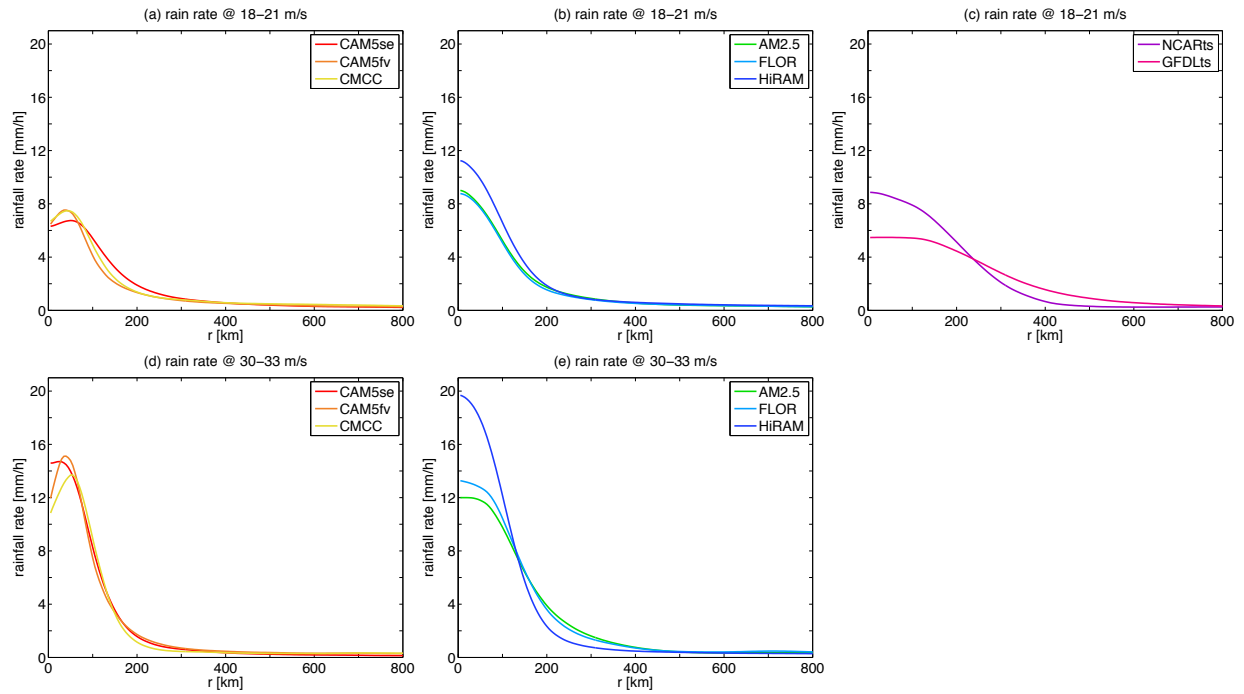


Figure 5: Azimuthally averaged rainfall rates for TC snapshots that have the intensity of (top) 18-21 and (bottom) 30-33 m s^{-1} . The left, middle, and right columns are the 0.25°, 0.5°, and 1° simulations, respectively.

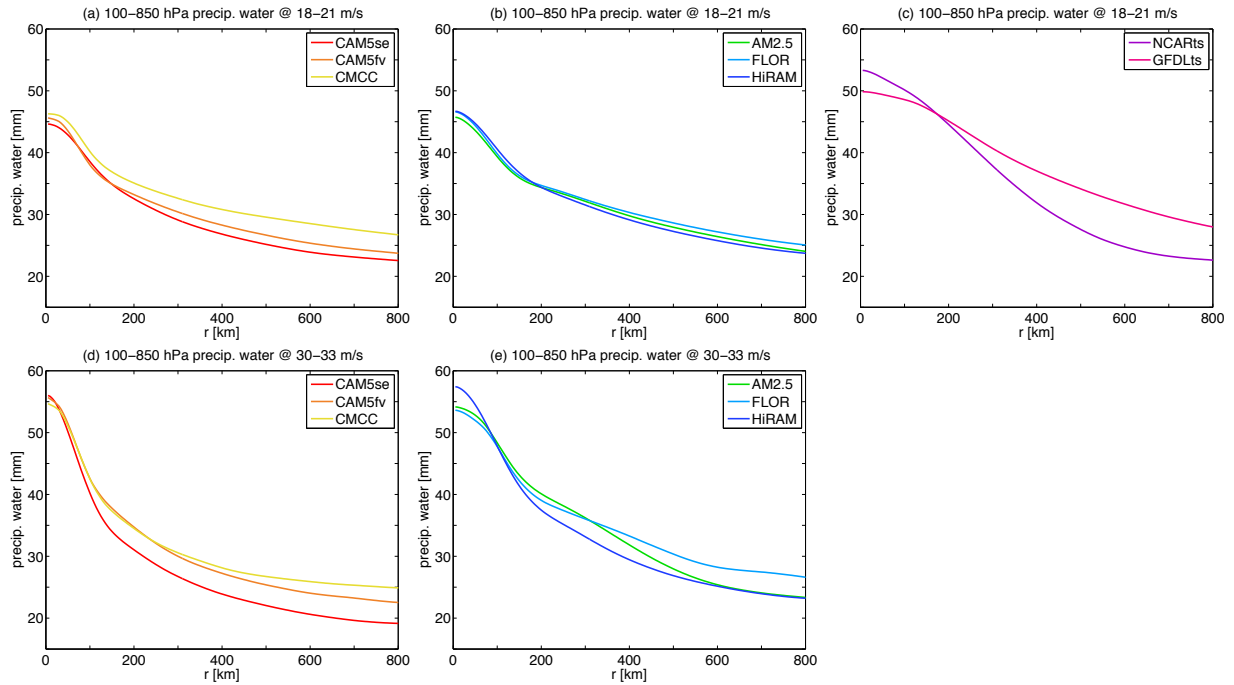


Figure 6: Azimuthally averaged 100-850 hPa precipitable water for TC snapshots that have the intensity of (top) 18-21 and (bottom) 30-33 m s^{-1} . The left, middle, and right columns are the 0.25°, 0.5°, and 1° simulations, respectively.

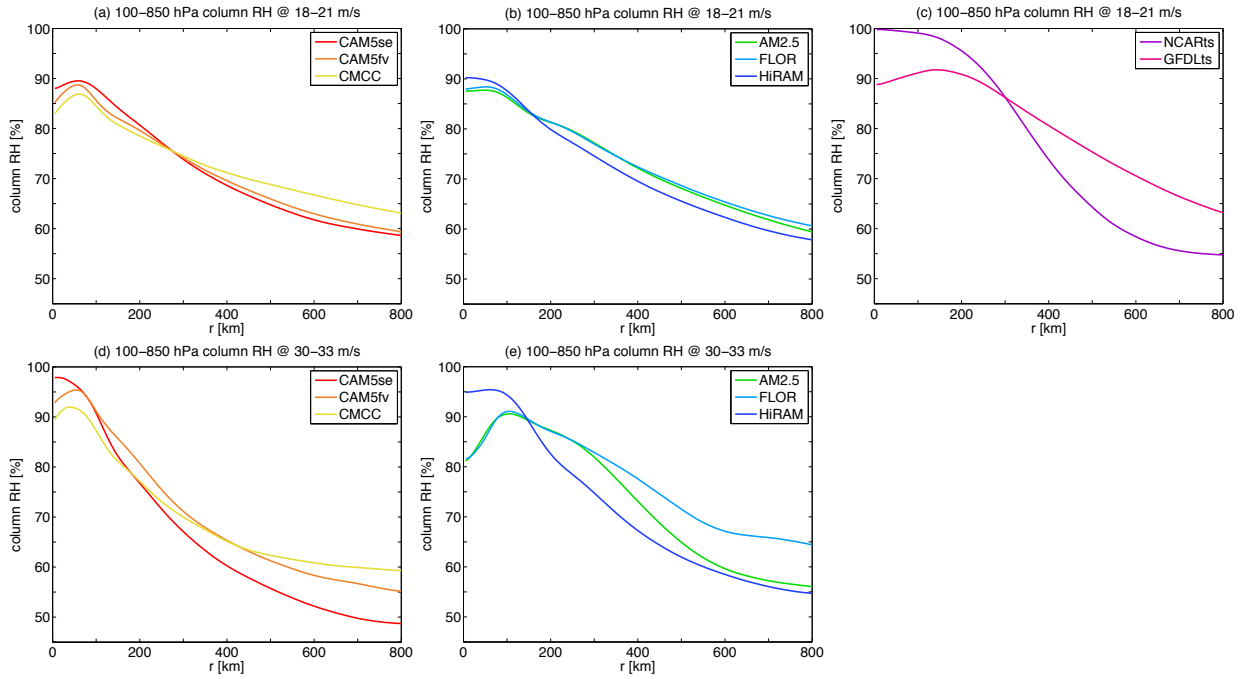


Figure 7: Azimuthally averaged 100-850 hPa column relative humidity for TC snapshots that have the intensity of (top) 18-21 and (bottom) 30-33 m s^{-1} . The left, middle, and right columns are the 0.25°, 0.5°, and 1° simulations, respectively.

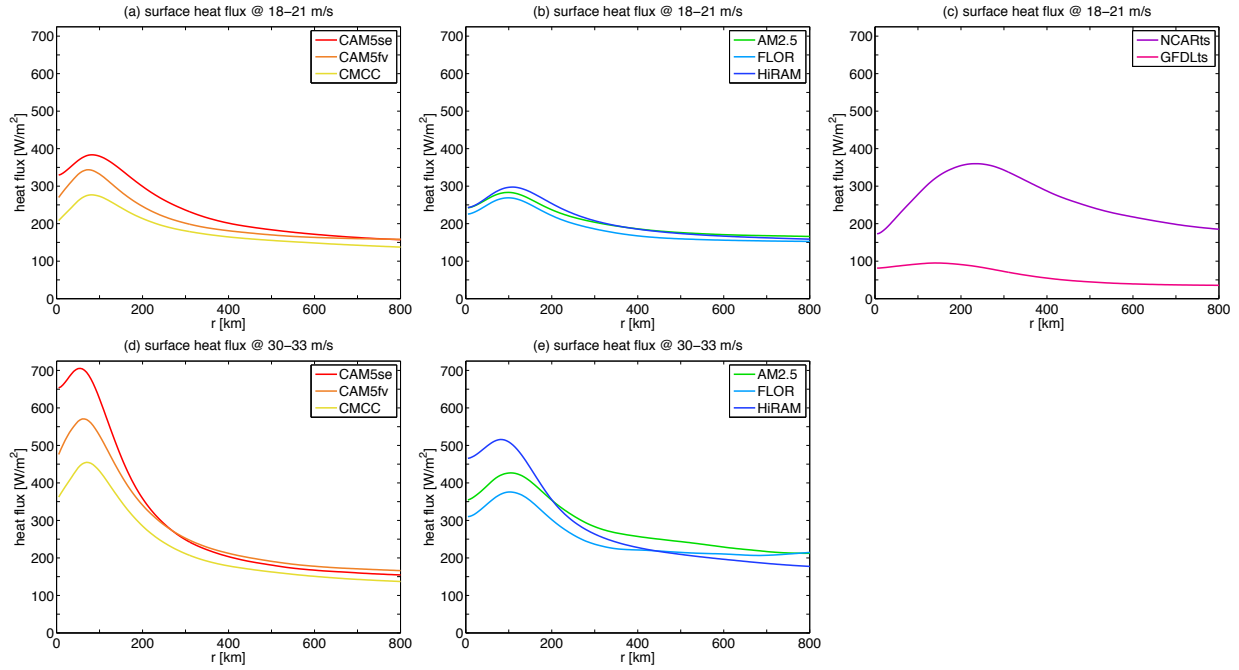


Figure 8: Azimuthally averaged surface heat fluxes for TC snapshots that have the intensity of (top) 18-21 and (bottom) 30-33 m s^{-1} . The left, middle, and right columns are the 0.25°, 0.5°, and 1° simulations, respectively.

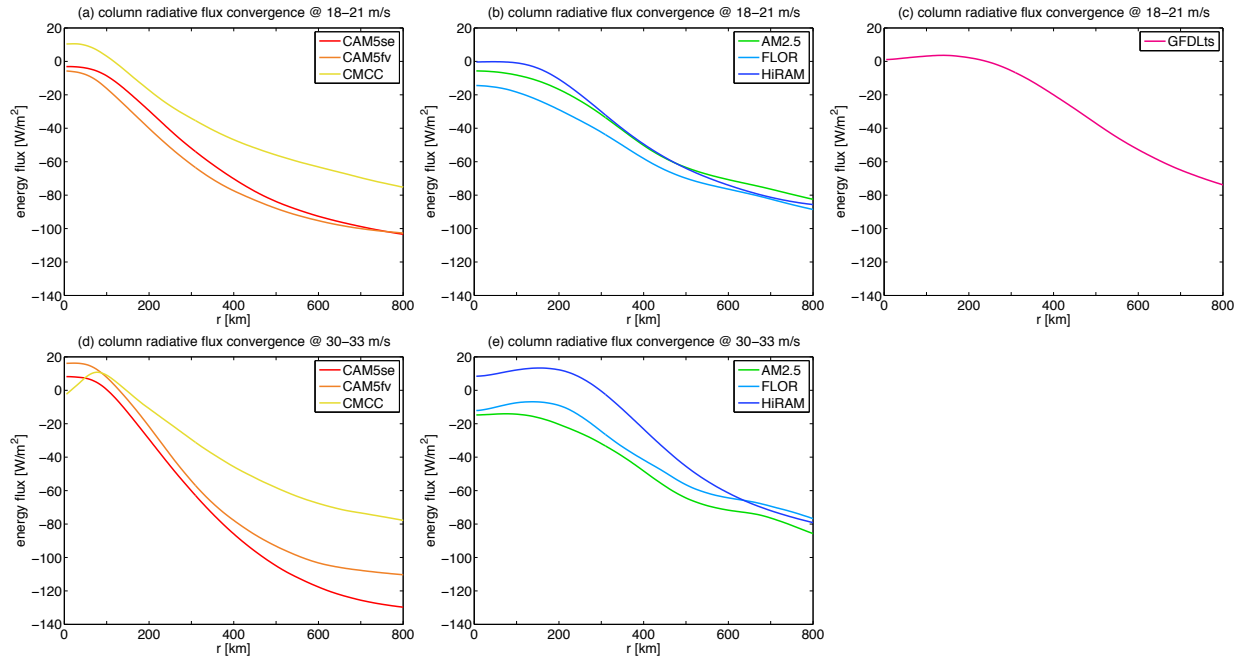


Figure 9: Azimuthally averaged net column radiative flux convergence for TC snapshots that have the intensity of (top) 18-21 and (bottom) 30-33 m s^{-1} . The left, middle, and right columns are the 0.25°, 0.5°, and 1° simulations, respectively.

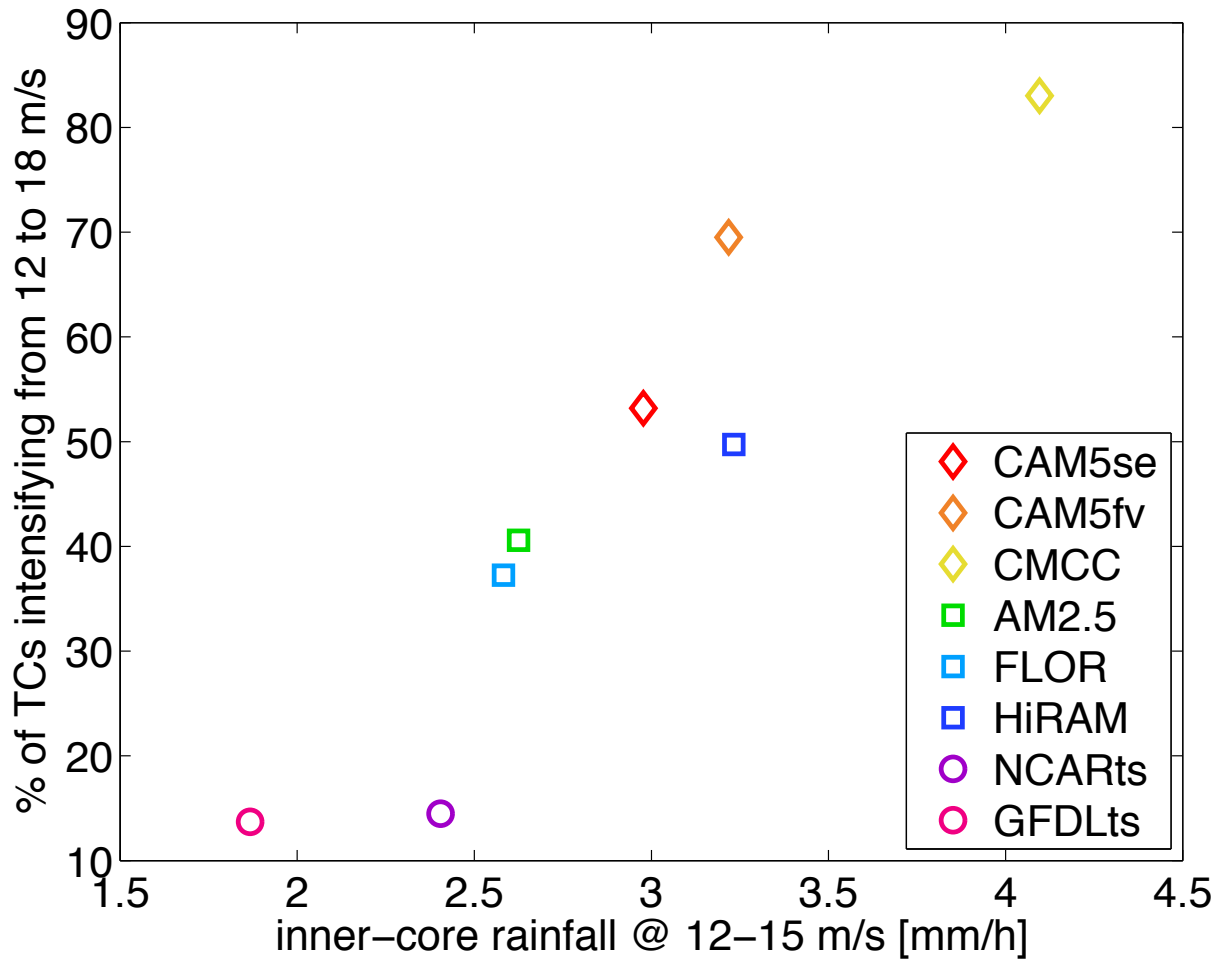


Figure 10: Scatterplot of the area-averaged inner-core rainfall rates at 12-15 ms^{-1} vs. the fraction of TCs intensifying from 12 ms^{-1} to 18 ms^{-1} in all simulations. The inner-core region is defined to be 2 times the 850-hPa RMW. Diamonds, squares, and circles are for the 0.25°, 0.5°, and 1° simulations, respectively.